CFD ASSESMENT OF A CENTRIFUGAL COMPRESSOR STAGE OPTIMIZATION PROCESS

Gheorghe FETEA[1], Bogdan GHERMAN[2], Dan Niculae ROBESCU[3]

The paper presents numerical studies of the second stage of a centrifugal compressor which is part of industrial gas turbine. The numerical analysis performed on the baseline geometry identifies flow related problems in the rotor and the two diffusers. The optimization process aims to improve the performances by modifying the geometry of the three components, based on the results of the numerical analysis performed on the baseline. The numerical analysis presented here is a steady state simulation using the SST turbulence model, performed at the nominal regime.

Keywords: centrifugal compressor, industrial stage, steady – state, diffuser

Nomenclature

h specific enthalpy [*J/kg*]; *w*- molecular weight [*kg/kmol*]
p pressure [N/m^2]; *R*- universal gas constant [*J/kgK*]
T temperature [*K*]; *u* - velocity [*m*]; *t*- time [*s*]

Greek characters

δ Kronecker delta [-]; μ dynamic viscosity [*kg/*(*ms*)]

ρ density [kg/m^3]; τ_{ij} turbulent stress tensor [m^2/s^2]

Dimensionless numbers

Pr Prandtl number

Statistical quantities

ϕ' fluctuating part of variable ϕ

$\tilde{\phi}$ filtered variable ϕ; $\overline{\phi}$ time or ensemble average of variable ϕ

1. Introduction

The research concerns the field of high-pressure ratio, large capacity centrifugal compressors for turboshaft engines that are used for cogeneration applications. The trend in the development of these new turboshaft engines is to increase the specific power output while decreasing the weight and volume of the machine. These requirements lead to highly loaded compressor stages, where the relative Mach number locally exceeds unity. Furthermore, the reduction of the outer diameter and height of the impeller leads to an increase in the inlet

[1] PhD Student, University POLITEHNICA of Bucharest, Romania, email: gheorghe.fetea@comoti.ro
[2] Romanian Research & Development Institute for Gas Turbines – COMOTI, Romania
[3] Prof, Hydraulics Department, University POLITEHNICA of Bucharest, Romania

centrifugal impeller blade height causing the inlet boundary conditions to change from subsonic to the transonic regime. This might cause the appearance of shock waves in front, or over the blade body, especially close to the blade tip region. The existence of a shock wave on the blade body means that the boundary layer experiences an extremely high adverse pressure gradient, which causes the detachment of the boundary layer from the blade [1]. This detachment induces losses that affect the compressor performances. Also, for a transonic, highly loaded centrifugal compressor, the presence of a shock wave affects the leakage flow at the tip of the blade [5], while the presence of a vane diffuser might have a detrimental effect on the impeller leakage flow. Shum et. al [6] showed that an optimum radial gap providing an optimum pressure ratio exists. Also, the recirculation zones triggered by the boundary layer detachment have an important impact on the flow angle and compressor stability.

Following these ideas, this paper proposes a study of the second centrifugal compressor stage of an industrial gas turbine. The numerical analysis identifies the aerodynamical problems in the compressor stage, requiring further optimization. A CFD assessment study is carried out to show the impact of the optimization process on the performances of the compressor stage.

2. Mathematical Model

In order to asses the optimization process on the centrifugal compressor stage, the Reynolds Averaged Navier – Stokes (RANS) numerical approach was employed. In order to allow the assessment of the boundary layer behavior, the SST turbulence model was used [20, 21]. The flow is compressible, and the equations that govern the flow presented below, time and mass averaged: [4]

The Continuity Equation**:**

$$\frac{\partial \overline{\rho}}{\partial t} + \frac{\partial \overline{\rho}\widetilde{u}_j}{\partial x_j} = 0 \tag{1}$$

The Momentum Equations:

$$\frac{\partial \overline{\rho}\widetilde{u}_i}{\partial t} + \frac{\partial \overline{\rho}(\widetilde{u}_i\widetilde{u}_j)}{\partial x_j} = -\frac{\partial \overline{p}}{\partial x_i} + \frac{\partial}{\partial x_j}\left(\overline{\tau_{ij}} - \overline{\rho u_i' u_j'}\right) \tag{2}$$

where,

$\overline{\tau_{ij}} = \mu\left[\frac{\partial \widetilde{u}_i}{\partial x_j} + \frac{\partial \widetilde{u}_j}{\partial x_i} - \frac{2}{3}\delta_{ij}\left(\frac{\partial \widetilde{u}_k}{\partial x_k}\right)\right]$, represents the stress tensor.

The Total Energy Equation:

$$\frac{\partial}{\partial t}\left(\overline{\rho}\widetilde{h}\right)+\frac{\partial\left(\overline{\rho}\widetilde{u}_j\widetilde{h}\right)}{\partial x_j}=\frac{\partial\overline{p}}{\partial t}+\frac{\partial}{\partial x_j}\left(\overline{\frac{\mu}{\Pr}\frac{\partial h}{\partial x_j}}\right)+\overline{\tau}_{ij}\frac{\partial\widetilde{u}_j}{\partial x_j}+\frac{\partial}{\partial x_j}\left(-\overline{\rho h'u'_j}\right), \tag{3}$$

where h is the enthalpy.

Ideal Gas Equation of State:

$$\widetilde{\rho}=\frac{w\left(\widetilde{p}+p_{ref}\right)}{R_0\widetilde{T}} \tag{4}$$

where, w is the molecular weight.

The SST turbulence model is a two-equation model, and in this class the turbulence velocity scale is computed from the turbulent kinetic energy, which is provided by numerically solving its transport equation along with the governing equations presented earlier. [20, 21]

The convergence is considered satisfied when the following criteria are met:
- the residuals for pressure are under 1e-5;
- the inlet mass flow has the same value as the one from the outlet;
- the residuals do not decrease or increase anymore..

3. Problem setup and boundary conditions of the numerical simulations

The optimization process focused on the increase of efficiency while keeping unchanged the speed and the flow channel size and shape. The optimization process has been carried out based on the accumulated experience and the in-house codes developed at COMOTI [19, 20], but it is not the subject of this article. The computational domain for both cases is presented in Fig. 2. For each part of the compressor stage only one channel was modeled, and periodic boundary has been used for each sector. Table 1 presents the boundary conditions used and the geometry specifications.

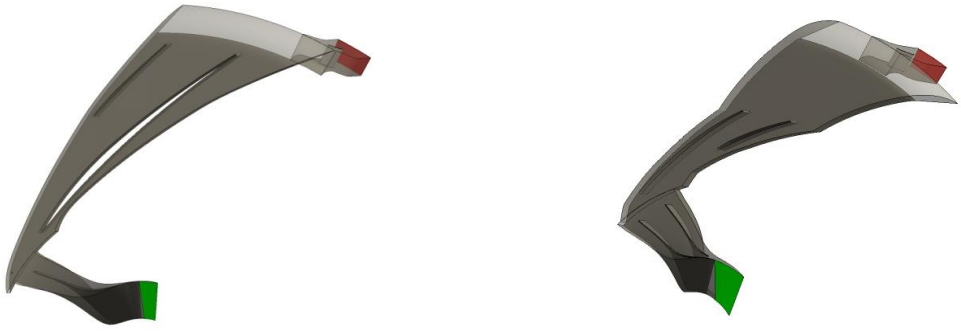

a b

Fig. 2 Computational domain, initial compressor stage (a) and optimized compressor stage (b)

Table 1

Stage geometry specifications

	Rotor	Optimized Rotor	Diffuser 1	Optimized Diffuser 1	Diffuser 2	Optimized Diffuser 2
Gas	Air		Air		Air	
Speed	22 000		-		-	
Mass flow rate	8.1 kg/s		8.1 kg/s		8.1 kg/s	
Pressure ratio	≈ 2.5					
Number of Blades	30	15	14	14	60	60
Number of splitters	0	15	14	14	-	
Total pressure at inlet	4.19 bar		-		-	
Total temperature at inlet	453.6 K		-		-	

The reference pressure is the atmospheric pressure, 1.01325 bar. At the exit, the mass flow rate is 8.1 kg/s / 60 blades = 0.135 kg/s. The solid walls were considered adiabatic (no heat transfer), impermeable and no-slip (zero velocity at the wall).

For both cases, a structured O-grid grid has been used to allow an efficient control of the grid size close to the walls, aiming for a $y^+ \sim 1$. The number of grid points for each part of the centrifugal compressor it is presented in table 2.

Table 2

Grid points distribution

Original compressor stage	Grid points
Rotor	873.920
Diffuser 1	639.600
Diffuser 2	460.800
Optimized compressor stage	Grid points
Rotor	1.546.803
Optimized Diffuser 1	870.400
Optimized Diffuser 2	611.520

4. Results and Discussion

The two cases that were studied concern the original geometry and the optimized geometry. The results presented in the following section will show on each part of the centrifugal stage a comparison between the two cases.

The first part of the centrifugal compressor analyzed is the rotor. In Fig. 3a a Mach 1 region can be observed close to the leading edge. During the optimization process, this region has been eliminated, Fig. 3.b. The Mach number reduces in the same region to a value of 0.6 – 0.7.

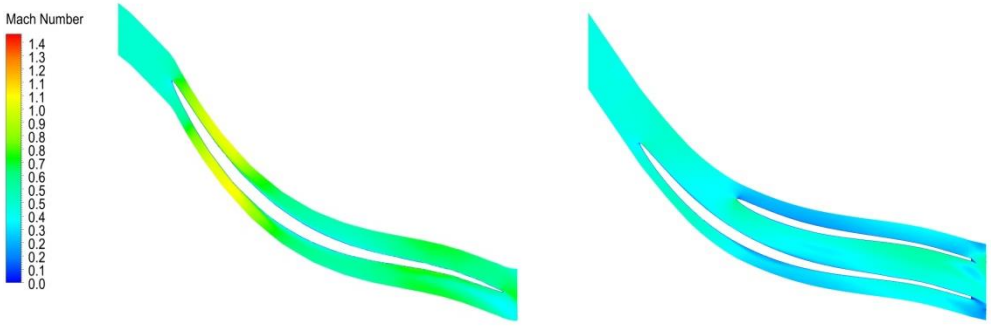

a b

Fig. 3 Relative Mach number, at 10% of blade height, measured from hub, original geometry (a) and optimized geometry (b)

In figure 4.a. it can be seen that the original rotor it is in transonic regime. The flow inside the optimized geometry is still in subsonic regime.

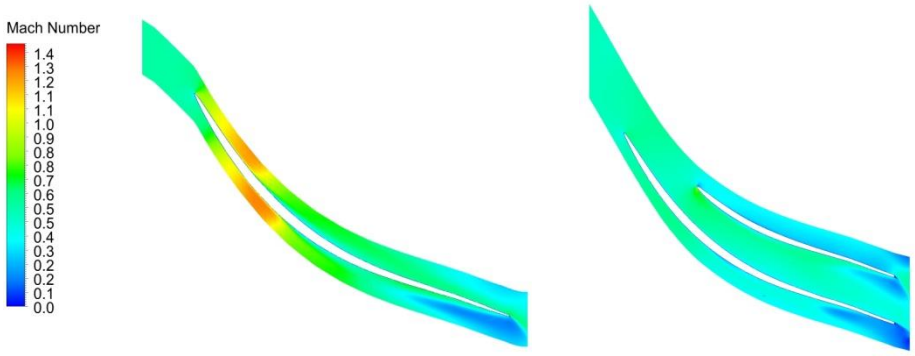

a b

Fig. 4 Relative Mach number, at 50% of blade height, measured from hub, original geometry (a) and optimized geometry (b)

At the tip of the blades, Fig. 5, the flow is influenced by the tip clearance leakage and the secondary flow that appears due to flow direction change from axial to radial. [22] In fig. 5.a. a shock wave can be observed close to the leading edge of the blade. The presence of shock wave produces the detachment of the boundary layer. The flow inside the optimized geometry removes the shock wave and the boundary layer detaches only due to tip leakage and secondary flow. The flow distortions can be observed in Fig. 6.

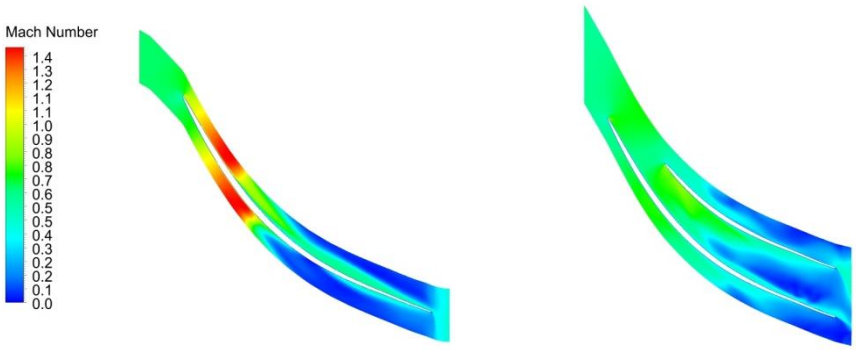

a b

Fig. 5 Relative Mach number, at 90% of blade height, measured from hub, original geometry (a) and optimized geometry (b)

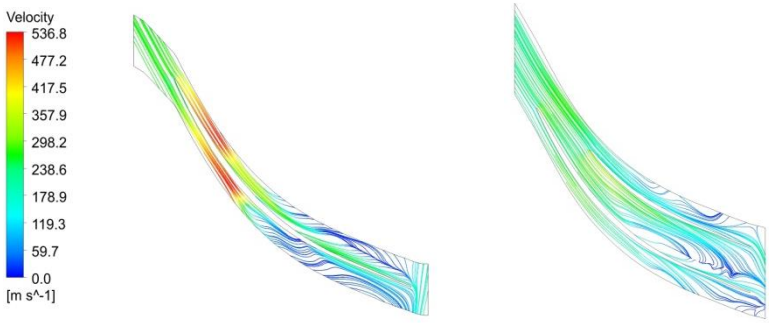

a b

Fig. 6 Stream lines at 90% from blade height, measured from hub, original geometry (a) and optimized geometry (b)

Another difference between the two cases it is seen at rotor efficiency, namely, the polytropic efficiency in the case of the original geometry is 93 % and the pressure ratio is 2.6; while in the case of the optimized geometry the polytropic efficiency remains 0.93 but, the pressure ratio increases to 2.65. This can be explained through the presence of the shock wave in the original geometry.

Fig. 7 shows the flow field inside the first diffuser, and the massive recirculation zone that occurs in the original geometry between blade and splitter. During the optimization process the recirculation zones have been removed, see Fig. 7.b.

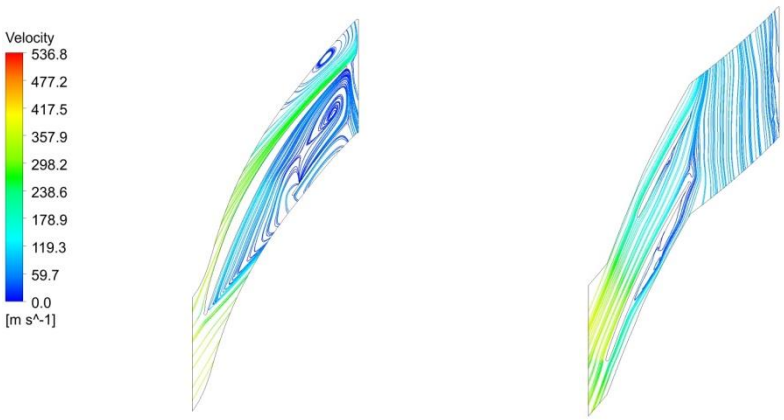

a b

Fig.7 Stream lines at 10% from blade height, measured from hub, diffuser 1, original geometry (a) and optimized geometry (b)

At the middle distance between hub and shroud it can be seen (Fig. 7.a. and Fig. 8.a.) that the space between the blade and the splitter is completely blocked. After optimization, the recirculation zone from the splitter has been completely removed and the one from blade was reduced, see Fig. 8.b. This modification of flow structure also influences the flow angle at the trailing edge of the diffuser section.

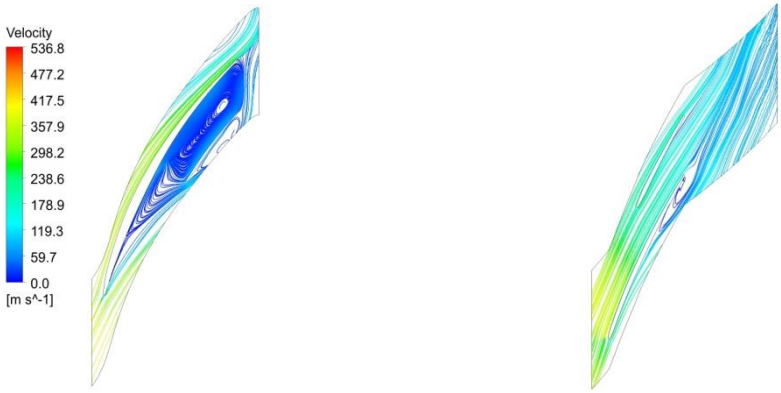

a b

Fig. 8 Stream lines at 50% from blade height, measured from hub, diffuser 1, original geometry (a) and optimized geometry (b)

In Fig. 9.a. the same recirculation zone that forms between blade and splitter can be observed. Here, practically the entire space from hub to shroud is blocked; see Fig. 7a, 8a and 9a.

a b

Fig. 9 Stream lines at 90% from blade height, measured from hub, diffuser 1, original geometry (a) and optimized geometry (b)

In the case of the second diffuser another recirculation zone can be observed close to the trailing edge. This vortex is present on the entire blade height (Fig. 10.a – 11.a). However, the optimization process could not change the flow structure in this case. However, the flow angle at the exit from the second diffuser is improved, recuperating more than 20 degrees. As mentioned before, this compressor is part of a gas turbine and the flow angle is important for the design of the combustion chamber.

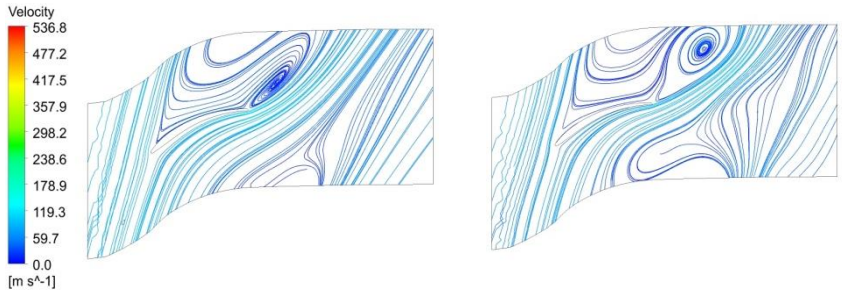

a b

Fig. 10 Stream lines at 50% from blade height, measured from hub, diffuser 2, original geometry (a) and optimized geometry (b)

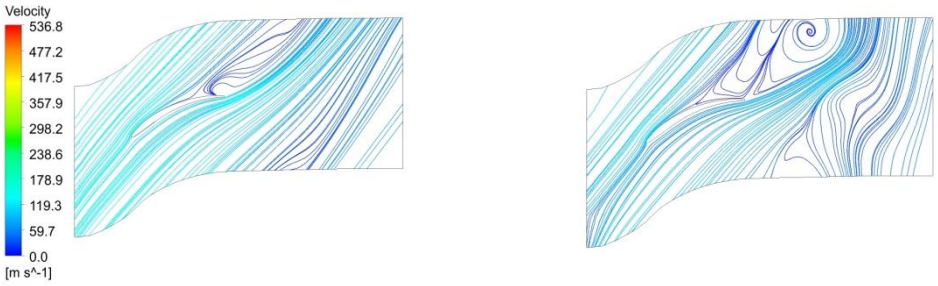

a b

Fig. 11 Stream lines at 90% from blade height, measured from hub, diffuser 2, original geometry (a) and optimized geometry (b)

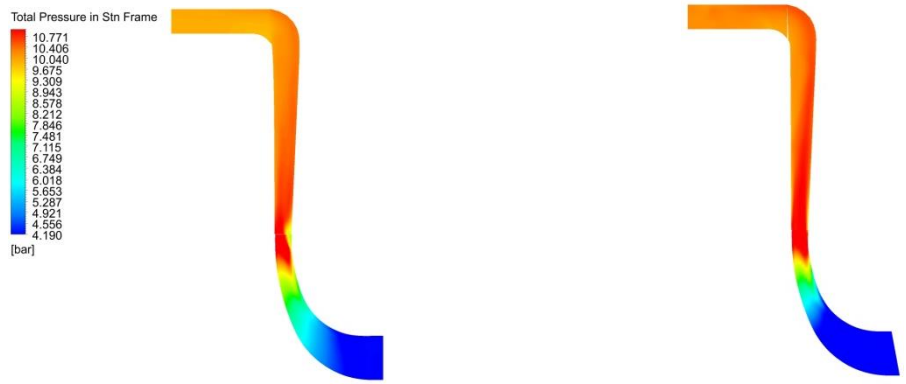

a. b.

Fig. 12 Meridional Total pressure distribution , from inlet to outlet , original stage (a) and optimized stage (b)

In Fig. 12 is presented the total pressure distribution on the meridional plane, from stage inlet to outlet. As it can be seen, there are some non - uniformities at the rotor exit in Fig. 12.a. However, the pressure distribution smoothens out in the diffusers section in both cases, towards the stage outlet.

In Fig. 12 is presented the total pressure distribution on the meridional plane, from stage inlet to outlet. As it can be seen, there are some non - uniformities at the rotor exit in Fig. 12.a. However, the pressure distribution smoothens out in the diffusers section in both cases, towards the stage outlet.

In Fig. 13, the pressure recovery achieved during the optimization process, of approximately 0.2 bars can be observed.

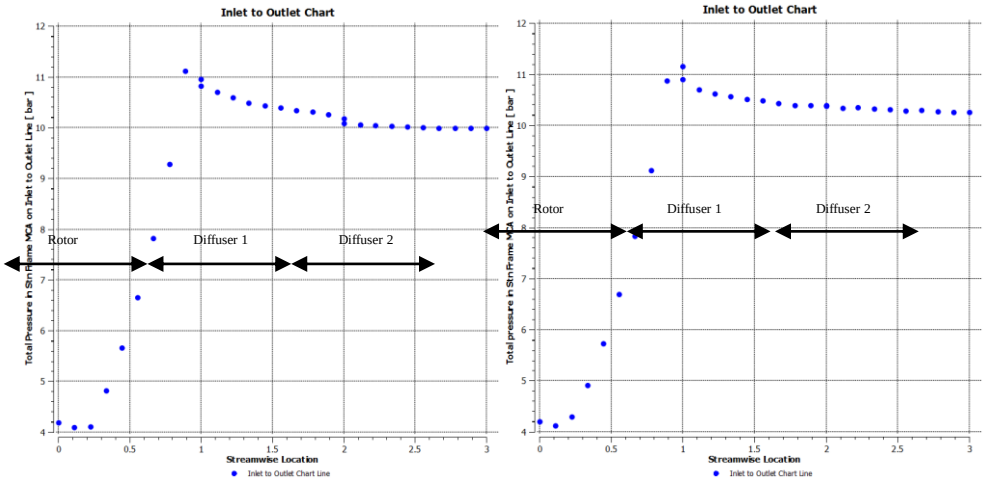

a b

Fig. 13 Total pressure distribution from inlet to outlet, original geometry (a) and optimized geometry (b)

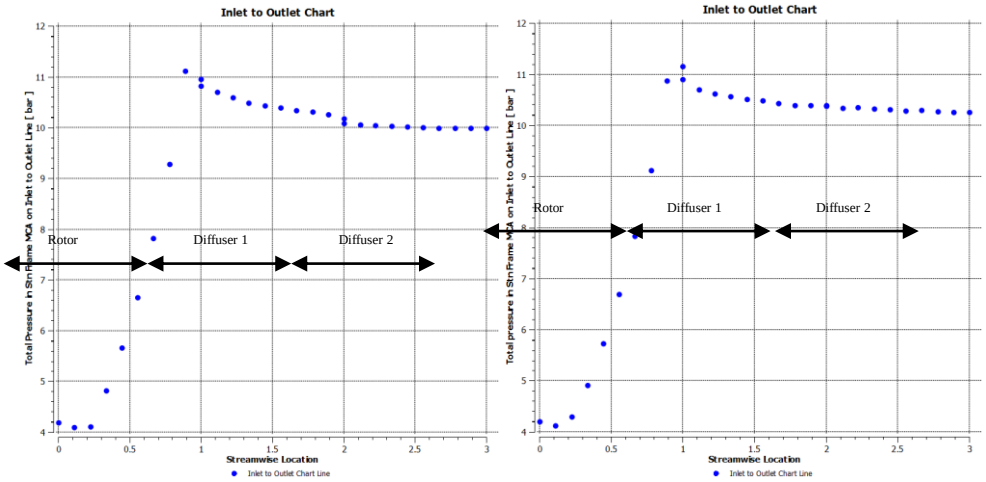

a b

Fig. 13 Total pressure distribution from inlet to outlet, original geometry (a) and optimized geometry (b)

Table 3

Performances obtained after optimization process

Parameter	Design point	Calculated using CFX	
Mass flow rate at nominal regime	8.1 kg/s	8.1 kg/s	
Pressure ratio at nominal regime	2.3	2.6	2.65
Polytropic efficiency at nominal regime : rotor / stage	80 %	93-81 %	93/86 %
Speed at nominal regime	22 000 rpm	22 000 rpm	
Total pressure at inlet	4.19 bar	4.19 bar	4.19 bar
Total pressure at rotor exit	10.07 bar	10.9 bar	11.1 bar
Total pressure at diffuser 1 exit	9.524 bar	10.1 bar	10.4 bar
Total pressure at diffuser 2 exit	9.515 bar	9.98 bar	10.2 bar

Also, the power consumed by the original stage is of 1365 kW and by the optimized geometry of 1297 kW. This difference it is important since these machines are working continuously.

5. Conclusions

In this paper, the second stage of a centrifugal compressor, part of an industrial gas turbine developed by INCDT COMOTI is studied. This second stage consists of a centrifugal rotor and two diffusers. In this analysis, the aerodynamic performances and losses pertaining to the original geometry are identified. The CFD analysis identified a shock wave that develops inside the rotor channel, close to shroud. Inside the first diffuser, a massive recirculation zone that closes the channel between the diffuser splitter and the blade is identified. In the second diffuser, a recirculation zone is identified at the trailing edge of the blade. These recirculation zones modify the flow angle and influence the combustion chamber design and performances. During the optimization process, it has been necessary to fulfill certain requirements: the flow path could

not be modified, the speed could not be modified, and the only thing that could be modified was the blades number, size, shape and angles. Taking this into consideration, the shock wave removal from the rotor channel leads to a subsonic flow that influences the boundary layer detachment and improves the flow angle at the rotor exit. The recirculation zone present between splitter and blade in the first diffuser has also been removed by modifying blades angles, shape and sizes. This leads to the improvement of the flow angle towards the exit. In the last diffuser, it was important to straighten the flow prior to combustion chamber.

To conclude, at the rotor, every second blade was cut, resulting 15 blades and 15 splitters. At the first diffuser, the blade angles, shape and size have been modified, and at the last diffuser only the blade angles have been modified. The assessment of the optimization process showed an increase in stage efficiency of 5 %, a reduction of the power consumption by almost 70 kW and a pressure ratio improvement of 2 %. Also, the flow angle at the exit of the compressor stage improves by 20 degrees.

R E F E R E N C E S

[1] *M.G. Hall*, Vortex breakdown, Annual Review of Fluid Mechanics, **vol.** 4: 195-218, 1972.

[2]*Ying Huang, Vigor Yang* - Dynamics and stability of lean-premixed swirl-stabilized combustion, Progress in Energy and Combustion Science, Volume 35, Issue 4, Pages 293–364, August 2009.

[3] *CFX Limited*, Waterloo, Ontario, Canada, *CFX-TASC flow Theory Documentation*, Section 4.1.2, Version 2.12, 2002.

[4] *John C. Tannehill, Dale A. Anderson, Richard H. Pletcher*, Computational Fluid Mechanics and Heat Transfer, second edition, 1997.

[5] *P. A. McMurtry, W. H. Jou, J. J. Riley, and R. W. Metcalfe*, Direct numerical simulations of a reacting mixing layer with chemical heat release, AIAA Journal, **Vol**. 26 No. 6, pag. 962 - 970, 1985.

[6] *Ko, S.C. and Sung, H.J.*, Large-eddy simulation of turbulent flow inside a sudden-expansion cylindrical chamber, Journal of Turbulence, 3, 011, 2002.

[7] *Szasz, R.Z., Duwig, C., and Fuchs, L.*, Numerical Simulation of reacting flows in Gas Turbine Burners with flame surface density model and LES, conference on Modeling Fluid flow (CMFF'03), Budapest, Hungary, September 3-6, 2003.

[8] *Gherman, B.G., Szasz, R.Z., Fuchs, L*., LES of Swirling flows in Gas Turbine combustion chambers, ASME Turbo Expo 2004, Vienna, Austria, June, 2004.

[9] *R.K. Cheng.*, Ultraclean low-swirl combustion will help clear the air. Personal communication and EETD newsletter, 2003.

[10] *G. Boudiera, L.Y.M. Gicquela, T. Poinsotb, D. Bissièresc, C. Bératc* - Comparison of LES, RANS and experiments in an aeronautical gas turbine combustion chamber - Proceedings of the Combustion Institute Volume 31, Issue 2, Pages 3075–3082, January 2007.

[11] *F. Wang, , L.X. Zhou, C.X. Xu* - Large-eddy simulation of correlation moments in turbulent combustion and validation of the RANS-SOM combustion model – Fuel Volume 85, Issue 9, Pages 1242–1247, June 2006.

[12] *Wei Wang, Tarek Echekki* - Investigation of lifted jet flames stabilization mechanism using RANS simulations - Fire Safety Journal Volume 46, Issue 5, Pages 254–261, July 2011.

[13] *V.L. Zimont, V. Battaglia* - Joint RANS/LES approach to premixed flames modeling in the context of the TFC combustion model - Engineering Turbulence Modeling and

Experiments 6 — Proceedings of the ERCOFTAC International Symposium on Engineering Turbulence Modeling and Measurements - ETMM6 -Sardinia, Italy, 23–25 May, 2005.

[14] *Khalid M. Saqra, Hossam S. Alyb, Hassan I. Kassema, Mohsin M. Siesa, Mazlan A. Wahida* - Computations of shear driven vortex flow in a cylindrical cavity using a modified k-ε turbulence model - International Communications in Heat and Mass Transfer, Volume 37, Issue 8, Pages 1072–1077, October 2010.

[15] *X. Bai & L. Fuchs* – Modeling of turbulent reactive flows past a bluff body: Assessment of accuracy and efficiency, Computers and Fluids, 23(3):507-521, 1994.

[16] *Kato, M., Launder, B.E.* - The modeling of turbulent flow around stationary and vibrating square cylinders - Ninth Symposium on "Turbulent Shear Flows", Kyoto, Japan, August 16-18, 1993.

[17] *F. C. Goldin, J.S. Depsky, S.L. Lee* – Velocity characteristics of a swirling flow combustor, AIAA journal, 23(1):95-102, 1985.

[18] *V. Tangirala, R. Chen, J.F. Driscoll* – Effects of heat release and swirl on the recirculation within swirl-stabilized flames, Combust. Sci. and Tech., 51:75-95, 1987.

[19] *M.L. Niculescu, V. Silivestru, G. Vizitiu, B. Gherman, S. Danaila*, C. Berbente - Detailed investigation of an atomizing air compressor, ISAIF8-00125, Proceedings of the 8th International Symposium on Experimental and Computational Aerothermodynamics of Internal Flows -July, Lyon, 2007.

[20] *B. Gherman, M. Draghici* – Centrifugal Blower Optimization, internal report, DT 5/11.04.2011, 2011.

[21] *Menter, F. R.*, Zonal Two Equation k-ω Turbulence Models for Aerodynamic Flows, AIAA Paper 93-2906, 1993.

[22] *Menter, F. R.*, Two-Equation Eddy-Viscosity Turbulence Models for Engineering Applications, AIAA Journal, vol. 32, no 8. pp. 1598-1605, 1994.

[23] *V. Dragan, B. Gherman, I. Malael, R. Bimbasa*, Global Analysis of Tip Clearance on Centrifugal Compressor, VOL. 811, PP 128-132, ICMERA, 2015.